We are IntechOpen, the world's leading publisher of Open Access books Built by scientists, for scientists

6,900
Open access books available

185,000
International authors and editors

200M
Downloads

Our authors are among the

154
Countries delivered to

TOP 1%
most cited scientists

12.2%
Contributors from top 500 universities



WEB OF SCIENCE™

Selection of our books indexed in the Book Citation Index in Web of Science™ Core Collection (BKCI)

Interested in publishing with us?
Contact book.department@intechopen.com

Numbers displayed above are based on latest data collected.
For more information visit www.intechopen.com



Chapter 3

Optimisation of Parameters for Spectroscopic Analysis of Rare Earth Elements in Sediment Samples

Martin Makombe, Charlton van der Horst, Bongiwe Silwana, Emmanuel Iwuoha and Vernon Somerset

Additional information is available at the end of the chapter

http://dx.doi.org/10.5772/intechopen.68280

Abstract

The rapid demand for rare earth elements (REEs) in recent years due to increased use in various technological applications, agriculture, etc. has led to increased pollution and prevalence of REEs in the environment. Therefore, monitoring for REEs in the aquatic environment has become essential including the risk assessment to aquatic organisms. Since direct determination of REEs in sediment samples prove difficult at times, due to low concentrations available and complex matric effects, separation and enrichment steps are sometimes used. In this work, various REEs were determined employing wet acid digestion and lithium metaborate fusion in our optimised analytical technique. A comparison of the two analytical techniques was also made. The results obtained from the optimised ICP-OES radial view technique were in 5% agreement with the ICP-MS results from the same samples. The accuracy of the method was checked with the geological reference material GRE-03 and found to be in reasonable agreement. We demonstrated that there is a consistent relationship between the signals of the REEs and nebuliser gas flow rates, plasma power and pump speed. The detection limits for all the REEs ranged from 0.06 mg L^{-1} Yb to 2.5 mg L^{-1} Sm using the ICP-OES fusion technique.

Keywords: rare earths elements, spectroscopy optimization, lithium metaborate, fusion digestion and sediment

INTECH
open science | open minds

© 2017 The Author(s). Licensee InTech. This chapter is distributed under the terms of the Creative Commons Attribution License (http://creativecommons.org/licenses/by/3.0), which permits unrestricted use, distribution, and reproduction in any medium, provided the original work is properly cited. CC BY

1. Introduction

Sediment forms the deposit of organic matter, silt, alluvium or sludge that settles at the bottom of a liquid. Water in rivers, wind and glaciers normally transports the sediment. The sediment forms the habitat of the aquatic ecosystem. Furthermore, it acts as a sink or source for metals that can contribute to biogeochemical processes that occur in the aquatic environment [1].

The nutrients may be either useful or harmful depending on the concentration. High concentrations of non-essential metals including rare earth elements (REEs) are toxic to the environment. In environmental impact studies, sediments play a crucial role in monitoring contamination levels. The elemental analysis of sediments and soils has become important in the environmental studies, particularly for the identification of the contaminants present in the matrix and the relative threshold levels of toxicity [2]. River and estuarine sediments can be used to assess the pollution level of heavy metals and REEs as the surface sediments interact with the water column and record the depositional pollution history.

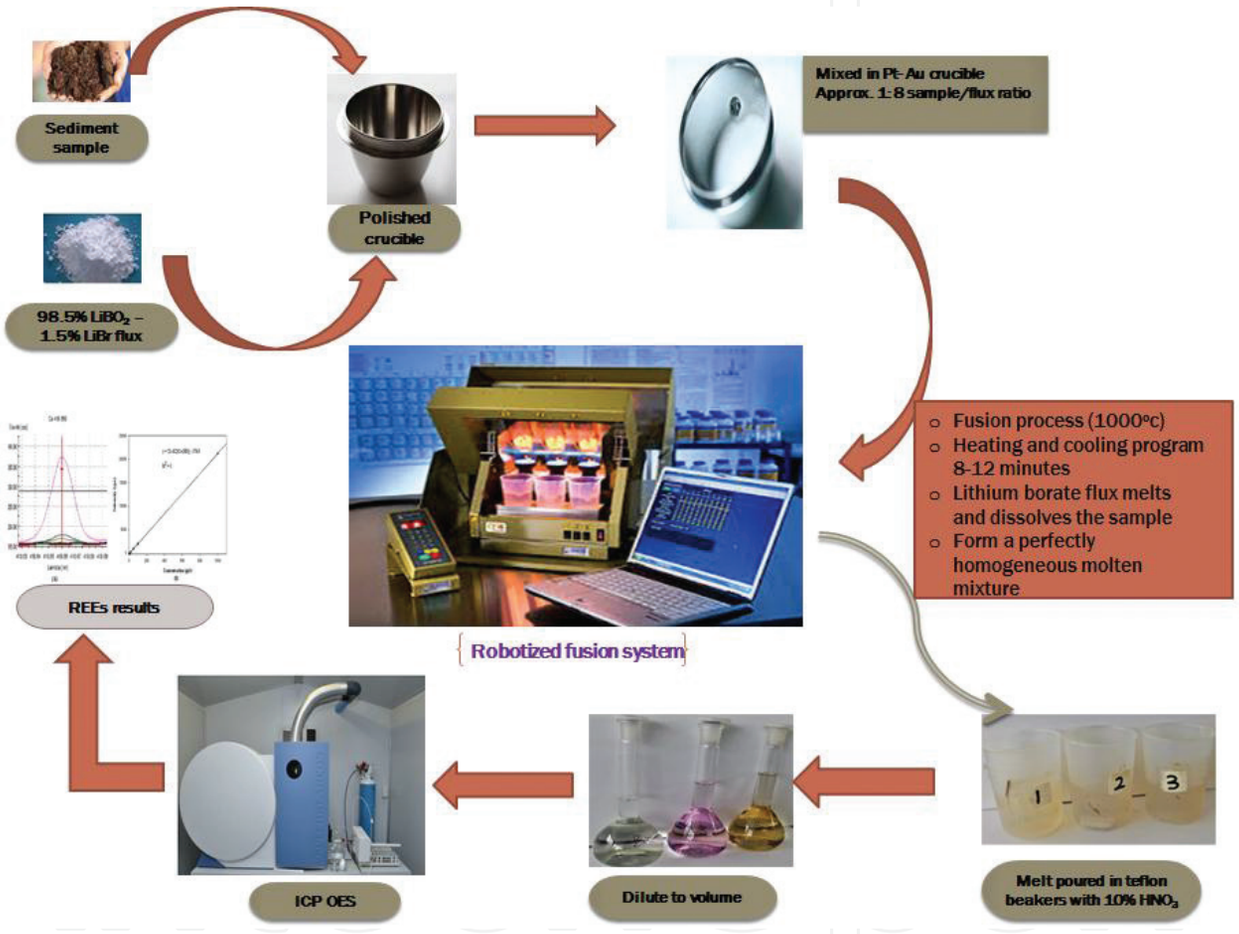
A major issue in the determination of soil elemental constituents is represented by the refractory nature of many metals including the REEs. Traditional methods for the analysis of REEs in sediments, based on instrumental techniques, require the complete dissolution of samples. Typically, this is done through alkaline fusion, microwave digestion and acid digestion on hot plates at atmospheric pressure. Following dissolution of samples, the spectrometric measurement is performed using different spectrometric techniques, such as flame atomic absorption spectroscopy (FAAS), graphite furnace AAS (GFAAS), neutron activation energy (NAE), X-ray fluorescence (XRF), inductively coupled plasma optical emission spectrometry (ICP-OES), or ICP mass spectrometry (ICP-MS). Although the procedures of acid solubilisation are effective, they are time-consuming and can often result in the loss of the most volatile species [3, 4].

A prerequisite for the determination of rare earth metals and other refractory elements, such as chromium, zirconium, barium, titanium, hafnium and strontium, is a complete sample digestion [5, 6]. This is a huge problem in many analytical laboratories as the process consumes time and sometimes requires costly equipment. The digestion of rare earth and refractory elements is commonly achieved using hydrofluoric acid (HF) in combination with mineral acids, such as nitric acid (HNO_3), hydrochloric acid (HCl) and perchloric acid ($HClO_4$) [7]. The HF is good on breaking up the silica matrix and to liberate all entrapped metals. The acid digestion procedures also often result in incomplete analysis of refractory and rare earth metals. In addition, the use of HF is extremely dangerous due to the reactive nature of the acid [8]. Li et al. [9] reported the digestion of sediment samples by microwave technique using HNO_3-H_2O_2-HF reaching detection levels of ng/L on ICP-MS. An alternative technique to the wet acid digestion procedure is the fusion method. This is achieved by mixing the sample with flux such as lithium, sodium and potassium borate fluxes. Occasionally $NaCO_3$, K_2CO_3, Na_2O_2 and NaOH fluxes may be used [10, 11]. The use of the flux-fusion approach is preferred due to the following reasons: (i) it is a complete digestion technique; (ii) it is much safer because HF is not used; (iii) the dominance of flux in solution results in similar matrix composition perfectly homogenous; (iv) it maintains constant grain size, thus the sample obtained will be

http://dx.doi.org/10.5772/intechopen.68280

almost perfectly homogenous; (v) the solutions are stable in dilute nitric acid and (vi) sample preparation time is shorter than that of the conventional acid digestions [10, 11].

The use of lithium metaborate ($LiBO_2$) as flux is similar to the XRF preparation of making fused beads, where total dissolution of sample is required. The key objective of this chapter is the determination of optimum instrument parameters and sample preparation conditions for ICP-OES analysis. Thus, this will facilitate very precise, accurate and rapid measurements of rare earth elements in sediment samples. Two different procedures used in this chapter for sediments decomposition were open-vessel wet digestion and lithium tetraborate fusion techniques [5, 6, 12].



Scheme 1. Schematic diagram showing the steps involved in fusion dissolution and analysis steps for a sediment sample (Adapted from, Boumans, 1987).

2. Materials and methods

2.1. Sediment sample preparation by fusion for ICP analysis

Upon arriving at the laboratory, the samples are kept frozen to minimise the potential for volatisation or biodegradation between sampling and analysis. The preparation of sediment

samples for chemical analysis collected from streams, rivers, ponds, lakes and oceans involves some steps to obtain a well-represented portion. Samples are first screened to remove foreign objects and large particulates, dried at 70°C and split to retain a fraction for storage. The chemically active fraction of sediment is usually cited as that portion which is smaller than 63 mm (silt + clay) fraction [13]. All weights were measured on a five-digit analytical balance (Mettler model).

A control sample can be prepared from portions that have been analysed. Thus, such finished material should be combined and well mixed into a larger storage container for future use as control sample that monitors the extraction process. Recovery test of the control and any reference material is evaluated after each run.

2.2. Wet digestion technique

For the wet digestion procedure, a mixture of HCl, HF HNO_3 and $HClO_3$ is added sequentially to the sample. All chemicals used for the preparation of standards and reagents were of analytical pure grade purchased from Merck (South Africa). The ideal sample weight for optimum dissolution is between 0.25 and 1.0 g weighed in Teflon beakers. For this procedure, HCl was boiled to near dryness. The sample was soaked with 1:1 HF and HNO_3 for 8 h or overnight at room temperature to enhance dissolution and then boiled to near dryness. A 1:1 mixture of HNO_3 and $HClO_3$ was boiled until all white dense fumes disappeared and this stage drove off all HF remaining. Another boiling of HNO_3 followed by 10% HNO_3 v/v to redissolve all salts completed the dissolution stage. After cooling, the sample was transferred to 50 ml volumetric flask and topped with 10% HNO_3 v/v. Mixing of the sample was achieved by vigorous shaking, and the clear solution was transferred to a glass vial for ICP-OES analysis [9, 14].

2.3. Lithium metaborate fusion technique

The lithium metaborate dissolution procedure comprises the powdered sample mixed with flux of high purity in a desired proportion. The sediments that have organic matter and volatile phases are first ignited to fully oxidise the matter. However, the loss on ignition (LOI) can result in some loss of alkali metals; therefore, it was avoided in this study and, again, the sediments analysed had minimum volatile matter. The accurately weighed sample and flux is heated to approximately 1000°C on an automated fusion fluxer machine. The temperature is controlled by the gas flow that can be increased or reduced. The optimum temperature will melt and dissolve the sample to a perfectly homogeneous mass. Upon completion of the dissolution stage, the molten mixture is poured into heat-resistant Teflon beakers containing 100 mL of 10% v/v HNO_3 or as per dilution of choice for ICP analysis. Alternatively, the molten solution is poured into a preheated mould to produce a glass disk for XRF analysis [11].

Basically, the standard fusion process consists of the following three steps: (i) melting the sample/flux mixture; (ii) pouring the molten glass into an acid solvent; and (iii) dissolution of the molten glass into solution [15, 16]. The three steps play a huge significance in optimisation of the fusion technique. If one or more of the steps are not properly adhered to, then incorrect results and poor precision is obtained. The sample to flux ratio is essential in making sure that the entire sample is thoroughly dissolved in solution but avoiding flux saturation.

2.4. Fusion instrumentation, borate-fused fluxes and platinum accessories

The complete fully automated M4 fusion instrument (Corporation Scientific Claisse Inc, Canada), a three-position automatic gas instrument, was used in this study. Different borate fluxes were tried and the lithium metaborate (98.5% $LiBO_2$–1.5% LiBr) was the best, due to higher solubility and faster crystallisation during cooling. The high-purity borate fluxes are fused and consist of homogenous, spherical and vitreous particles, which are water-free and non-hygroscopic. To avoid wetting of the crucibles, a pre-mixed flux with a non-wetting agent was employed. The halogenated compounds of iodine and bromine were used to make halo acids, for example, LiI, LiBr, NaBr, KI and so on, as they produce good releasing agents. Claisse's type crucibles used were of exceptional quality, made of 95% platinum alloyed with 5% gold. It is highly recommended to mirror-polish the crucibles to retain flat and smooth surfaces to aid easy transfer of the melt into the acid ICP mixture [11]. All the fluxes used and platinum ware were purchased from Claisse (Canada).

2.5. Dilution for ICP analysis

The dissolution procedure for flux-fusion preparation of sediments results in an aqueous solution that can be analysed in a single analytical session for REEs, major and trace elements. Most sediments contain trace amounts of REEs depending on the sampling site and level of pollution from anthropogenic sources. It is suggested that the minimum or optimum dilution be performed to get low detection limits and precise results be employed. The salt content in the solution requires a dilution that does not affect the mobility of the sample on the ICP instrumentation. Too viscous solution of the alkaline salt tends to deposit salts on the ICP torch and clogging of the nebuliser [17]. Different dilutions can be prepared, if the overall goal of generating enough analyte at an appropriate concentration is fulfilled. A 500 times (nominal) dilution of sample was considered safe in sediments analysis giving acceptable detection limits.

2.6. ICP-OES instrumentation

The Spectro Arcos ICP-OES (SPECTRO Analytical Instruments GmbH Boschstrasse 10, Germany) equipped with smart analyser software was initialised for about 20 min before analysis to get stable plasma. All standard solutions were prepared from high-purity 1000 mg/L ICP-grade standards. The Spectro Arcos ICP-OES is equipped with charge coupled device (CCD) detectors and side-on plasma interface (SPI) or commonly known as radial that provides high precision and stability for less sensitive requirements [18]. The sample injection mode was by continuous nebulisation, and the signal processing or line measurement was based on the peak height. Polynomial plotted mode corrected the background. The ICP-OES analyses were carried out in controlled room of 20 ± 2°C. The results were verified for accuracy by an independent laboratory using ICP-MS (Thermo-Fisher X-Series II quadrupole ICP-MS with a New Wave UP213 solid-state laser ablation system). The spot size of the laser can be set to various diameters between 10 and 300 microns.

With ICP-OES analysis, the multi-elemental analysis using the simultaneous or sequential optical systems with radial viewing of the plasma is possible. To generate plasma for excitation, the argon gas is supplied to the torch coil and high-frequency electric current is applied to the

work coil at the tip of the torch tube. The high-frequency current generated by the electromagnetic field ionises the gas. When the excited atoms return to low energy position, emission rays (spectrum rays) are released, and the emission rays that correspond to the photon wavelength are measured. Samples are nebulised and the resulting aerosol is transported to the plasma torch in atomised state. Element-specific emission spectra are produced by radio-frequency (RF) inductively coupled plasma. Background correction is required for trace element determination. The ICP-OES measurement conditions need optimisation to get the best conditions for analysis, such as nebuliser flow rate, pumping speed, auxiliary and coolant flow rates and plasma power [19]. **Table 1** shows the optimised conditions for ICP-OES measurements equipped with a side-on plasma interface (SPI) or commonly known as radial [18]. ICP-OES and ICP-MS analyses are well regarded as appropriate environmental measurement techniques in measuring REEs, with the latter being more suitable for ultra-trace elemental levels [20]. Nowadays, due to the higher sensitivity achieved with axially viewed plasma and better spectral resolution given by high-resolution monochromators, it is expected that low concentrations of all naturally occurring lanthanides may be directly quantified by ICP-OES analysis [17].

Nebuliser type	**Crossflow**
Plasma power	1400 W
Torch	Demountable with alumina injector
Torch position	0
Nebuliser flow rate	0.8 L/min
Plasma flow rate	14.0 L/min
Auxiliary flow rate	2.1 L/min
Pump rate	40 rpm
Integration time	28 s
Replicates	3
Viewing height	Optimised on SBR
Plasma view orientation	Radial
PMT voltage	650 V
Background correction	Polynomial
Resolution	8.5 picometre
Detector	29 linear CCD

Table 1. Instrument operating conditions for the spectroscopic analysis of REEs.

2.7. Integration time

The integration (read) time was optimised using the instrument auto-integration mode. This phenomenon will take a snapshot of the intensities of various lines to be measured before the

http://dx.doi.org/10.5772/intechopen.68280

actual readings commence. The trace rare earth elements in sediments require larger integration time due to their low intensities and thereby increasing sample throughput. Additionally, longer read times lower the detection limits by reducing the effects of noise. Higher intensities will require shorter read time to reduce memory effects [9, 17].

2.8. Calibration

The calibration standards were prepared by diluting the stock multi-elemental standard solution 1000 mg L^{-1} in 10% (v/v) HNO_3 and 1.5% w/v flux (1.5 g in 100 mL). The calibration curves for all the studied elements were in the range of 0.01–1.0 mg L^{-1}. External calibration strategy is preferred for analysis of larger number of samples whilst standard addition method is suitable for small batches of samples. To avoid bias in external calibration method, a perfect matrix match of standards and samples is a prerequisite. Affected to a lesser degree by changes of the matrix composition or the presence of easily ionisable elements, calibration functions with excellent linearity and correlation were obtained, even without the use of an internal standard and an ionisation buffer [9, 17].

2.9. Interferences

The emission intensities were obtained for the most sensitive lines minimum of spectral interference. The REEs have very complex emission spectra and are difficult to measure in the presence of one another at very high concentrations using ICP-OES analysis. For this reason, ICP-MS analysis is the preferred measurement technique, but it can be very costly. Nebuliser, chemical, ionisation and spectral interferences are all present in ICP systems, but spectral interferences are most prominent [21].

Spectral interferences are common in ICP analysis and result from the overlapping profiles of spectral and interfering lines. The stray light from line emission of high concentration elements or particulate matter from atomisation process gives rise to enhanced emission light. This phenomenon gives rise to background emission, which is unwanted signal in analysis. This can be compensated for by subtracting the background emission determined by measuring the emission level on the two sides of the analyte peak and subtracting their average from the peak value [22].

Spectral interferences are caused by background emission from continuous or recombination phenomena, stray light from the line emission of high concentration elements, overlap of a spectral line from another element or unresolved overlap of molecular band spectra. Background emission and stray light can usually be compensated for by subtracting the background emission determined by measuring the emission level on the two sides of the analyte peak and subtracting their average from the peak value [22].

Figure 1 shows an example of the position of the atomic absorption peak and the background peak, as obtained for unidentified element. Spectral overlaps may also be avoided by using an alternate wavelength or can be compensated by equations that correct for inter-element contributions.

Nebuliser interferences, commonly known as matrix effects, arise from physical and chemical differences between analytical standards and samples. The inconsistent presence of matrix salts, different viscosities and surface tension of the liquid between the samples are

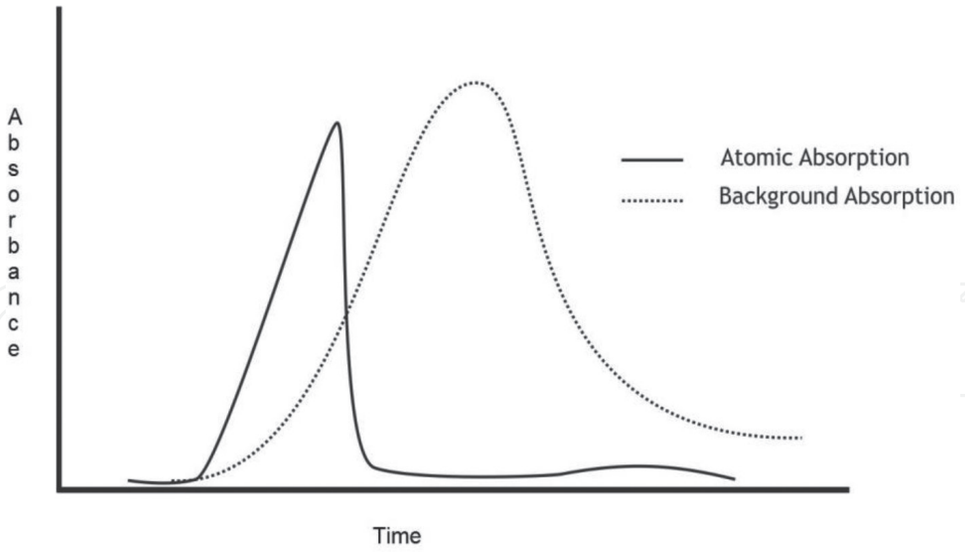


Figure 1. The position of the atomic and background absorption peaks that may cause spectral overlaps and contribute to inter-element interferences.

common problems of nebuliser interferences. The high salt content used in fusion technique needs to be diluted to avoid these interferences and match matrix of standards and samples. Using a high-solid nebuliser, the use of peristaltic pump can also reduce nebuliser interference [23].

2.10. Analytical wavelengths selection

Several criteria were applied for the selection: sensitivity (intensity of the line), selectivity (lack of interferences of other lines) and limits of detection (LOD). All selected lines were tested by using individual 0.1 mg L^{-1} REEs standard solutions in 10% HNO_3–$LiBO_2$ solution, searching the peak-centre in a first step. The optimised results obtained for ICP-OES analysis are shown in **Table 2**. Wavelength selection is somewhat of an individual choice that commonly varies from analyst to analyst and matrix of samples. However, there is a developing consensus regarding the wavelengths best suited for a target analyte [17, 21].

2.11. Detection limits

Method detection limits (MDL) for each element were calculated and are shown in **Table 2**. For comparison purposes, the LODs obtained using multi-acids and fusion dissolution for ICP-OES analyses are also shown. Validation was performed in terms of limits of detection (LOD), limits of quantification (LOQ), linearity, precision and recovery test. Lacking a suitable certified reference material, trueness was estimated using the recovery rate on fortified samples. Standards and blanks should be prepared using the same $LiBO_2$ strength and acids used for the samples and should be spiked with NIST traceable single and multi-element standards. The whole procedure should also be checked with certified reference material like the Geostart GRE-03 used in this study to ensure accuracy. The method detection

http://dx.doi.org/10.5772/intechopen.68280

Element (ppm)	Line (nm) [ICP-OES]	MDL (mg L^{-1}) (Acid digestion)	MDL (mg L^{-1}) (Fusion digestion)
La	333.749	1.1	0.3
Ce	418.660	1.6	1.0
Pr	417.939	1.2	1.4
Nd	430.358	2.4	2.1
Sm	360.428	2.8	2.5
Eu	420.505	0.8	0.1
Gd	335.862	1.1	0.7
Tb	231.890	2.3	1.9
Dy	338.502	1.4	0.7
Ho	345.600	0.8	0.3
Er	349.910	0.5	0.2
Tm	313.126	0.5	0.3
Yb	369.419	0.1	0.06
Lu	261.542	0.1	0.04
Y	371.030	0.1	0.08

Table 2. Wavelengths used and detection limits obtained for the use of acid and fusion digestion methods in ICP-OES analysis.

limits (MDLs) were calculated based on relative standard deviation (RSD) of 10 consecutive measurements of the matrix blank. The signals to background ratio, background equivalent concentration (BEC) and LOD were calculated according to the three equations provided below [24–26]:

$$SBR = \frac{[\,Int(standard) - Int(spectral background)\,]}{Int(spectral background)} \quad (1)$$

$$BEC = \frac{C(standard)}{SBR} \quad (2)$$

$$C_{DL} = 3 \times RSD_b \times \frac{BEC}{100} \quad (3)$$

where

RSD_b is the relative standard deviation of spectral background intensity (10 replicates of blanks); *C* is the concentration of the standard; SBR is the signal to background ratio and BEC is the background equivalent concentration.

3. Results and discussion

3.1. Sample-flux ratio optimisation

The influence of the flux/sample ratio on the concentration of the REEs is illustrated in **Figure 2**. The weight of the sample was examined from 0.100 to 0.300 g. The flux was varied

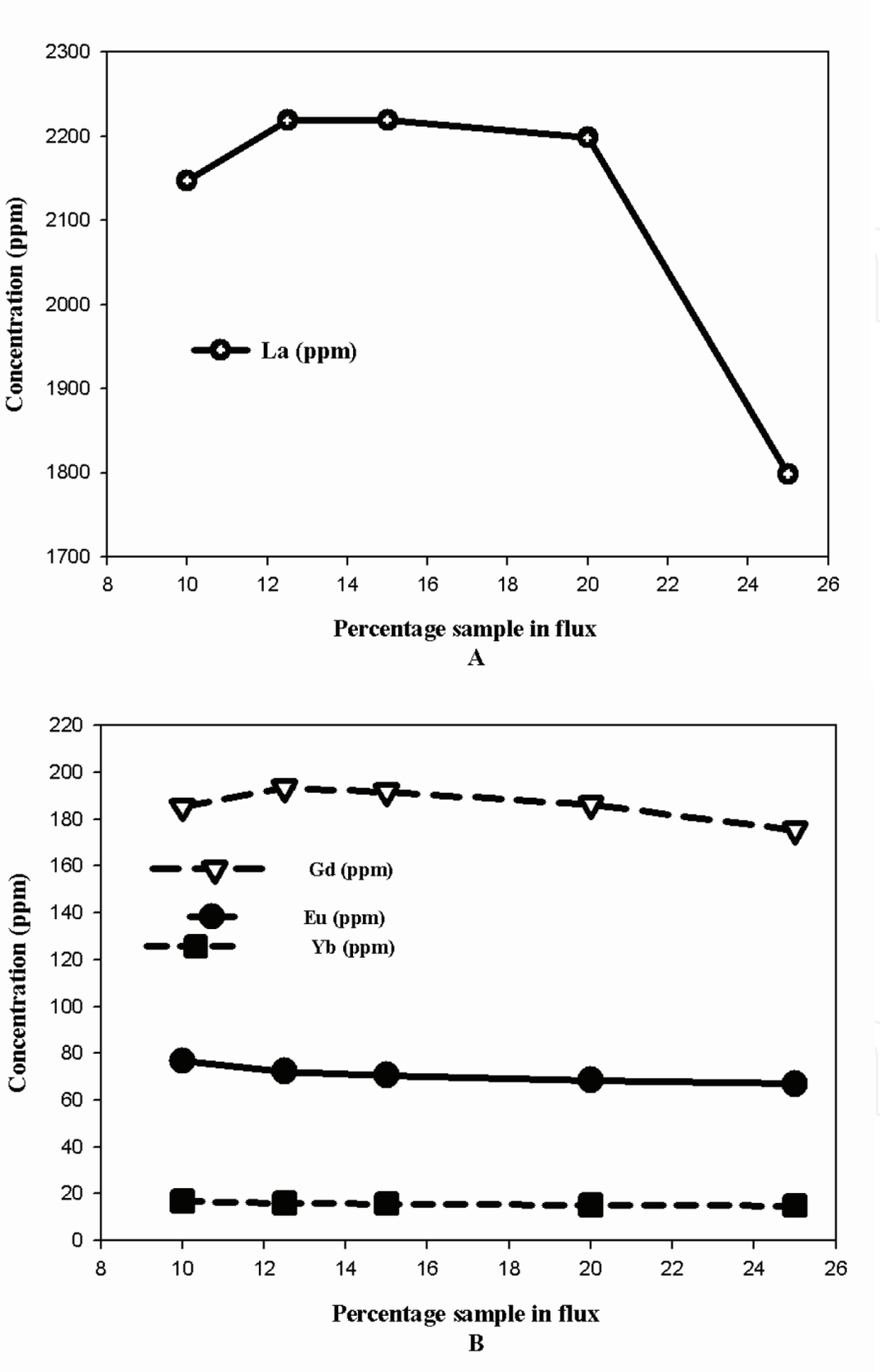


Figure 2. The effect of percentage of sample in flux (sample/flux ratio) on the concentration of La(II) (A) and Gd(II) and Eu(II) and Yb(II) (B) on GRE-03 reference material.

http://dx.doi.org/10.5772/intechopen.68280

from 1.00 to 3.00 g. In most fusion techniques, a ratio of 1:10 sample/flux mixture is considered optimum for making fused beads. The best concentration of the reference material at different sample/flux ratio for lanthanum is 12% or 1:8 ratio. In **Figure 2(A)**, the results are showed for lanthanum and 2(B) for gadolinium, europium and ytterbium that were found to be best between 12 and 14%. High sample flux ratio may cause the sample not to be fully dissolved especially with the presence of refractive elements [16]. The flux content should be enough to fully dissolve the sample, but care is needed not to have too much of the flux as it will increase deposits on the ICP torch.

3.2. The effect of nebuliser gas flow rate

Figure 3 shows the results obtained for the behaviour of the four elements at selected wavelengths as a function of the nebuliser gas flow rate. The rare earth elements not only have extremely similar chemical properties but also have inner abundance differences among them that provide different responses to applied parameters [27].

The intensities of wavelength of the REEs, whether at first (5.3–6.2 eV) or second (10–12 eV) ionisation state, are all similar. The REEs possess soft ionic wavelengths allowing second ionisation potentials [28].

The classification of wavelengths is necessary as the effect of different operating parameters on analytical performance depends on them. Each nebuliser has got its own optimum gas flow that directly controls the sample uptake en route the plasma. The longer the sample interacts in the plasma, the more optical transitions of the elements are possible by it acquir-

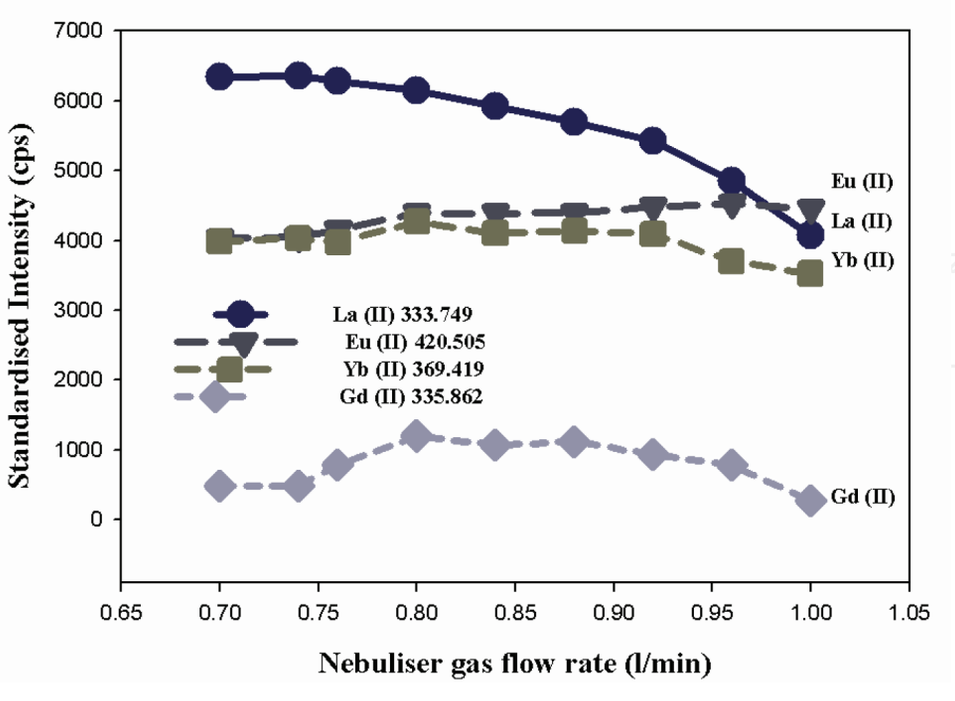


Figure 3. The effect of nebuliser gas flow on 0.1 mg L^{-1} of La(II), Yb(II), Eu(II) and Gd(II) standardised intensity counts, with the plasma power kept at 1300 W and pump speed at 35 rpm.

ing the energy for high energy interactions [29]. High nebuliser gas flow rate gives rise to reduced plasma temperature and lowers the atomisation. The low concentration of 0.1 mg L^{-1} of the REEs in $LiBO_3$–10% v/v HNO_3 was used for optimisation purposes.

The majority of the REEs studied to date gave best intensities at flow rates less than 0.82 L/min with La(II) [333.749] the lowest at 0.74 L/min [17]. An average flow rate at 0.80 L/min was chosen as the optimum nebuliser condition for all the rare earth elements studied.

3.3. The effect of plasma power

Power levels are critical when establishing optimum operating conditions. Higher power generates high temperature plasma conditions that lead to increases in intensity for atomisation and ionisation. The plasma power can have a major effect on the formation of oxides of lanthanides as well as in emission intensity and plasma robustness. Robust conditions of the plasma have been associated to high applied power by radiofrequency (RF) generator. **Figure 4** shows the results obtained for intensity measurements as a function of the RF power level for the four lines: La(II) [333.749], Eu(II) [420.505], Gd(II) [335.862] and Yb(II) [369.419] [17].

The standardised intensity rises with increased power levels due to the high energy of the plasma at higher power levels. The high plasma power also increases the background levels and sometimes at a rate higher than what the analyte increases. This rise indicates that the monitoring of background signal is important. On that instance, the best signal to background ratio needs to be established to get the optimum analyte signal and stable plasma. The standardised intensities rise with increase in RF power as shown in **Figure 4**. The plasma power

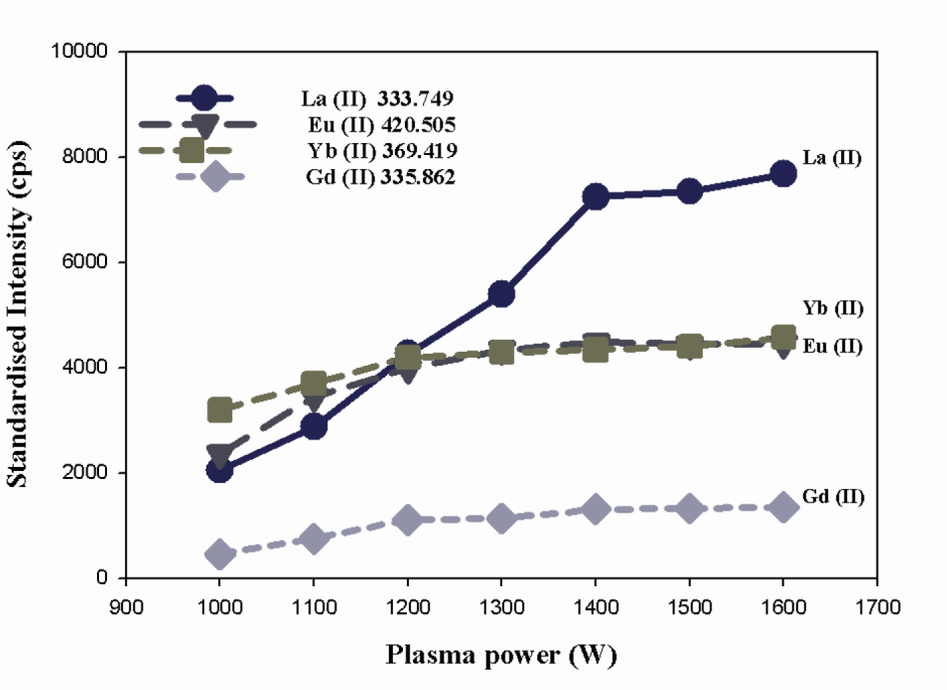


Figure 4. The effect of applied plasma power on 0.5 mg L^{-1} of La(II), Yb(II), Eu(II) and Gd(II) standardised intensity counts. The nebuliser gas flow rate was kept at 0.80 I/min and pump speed at 35 rpm.

http://dx.doi.org/10.5772/intechopen.68280

of 1400 W was chosen as the optimum condition for the analysis of trace rare earth elements in a salt matrix of lithium metaborate [17].

3.4. The effect of pump speed

The pump speed affects the uptake of sample and the efficiency of nebulisation that is very critical to sensitivity. The nebuliser gas pressure and the speed of the peristaltic pump determine the volume uptake of sample and both influence the sample transit to the plasma. Large sample volumes increase the background level due to poor aerosol formation in the spray chamber.

The type and dimensions of pump tubing have effect on the pumping speed; hence, the ideal tubing must be sought [9]. Lower pump speed or using narrow bore pump tubing will reduce uptake rate that is better for high %TDS samples and suitable for fusion samples. The ideal tubing should be resistant to the solvent in use and to withstand low to high acid concentrations.

Figure 5 shows the behaviour of the standardised intensity for the four elements, as a function of pump speed. The experimental results shown in **Figure 5** exhibit the increase in optical transitions of La(II), Yb(II) and Eu(II) with increase in pump speed up to about 35 rpm, and then a decline was observed. Gd(II) did not show many variations due to the pump speed. Once the optimum pump speed has been determined for a specific nebuliser and sample matrix, it does not have to be changed on an element-by-element basis. The pump speed of 35 rpm was considered optimum in this study. However, upon changing the sample matrix and type of nebuliser, the pump speed must be verified.

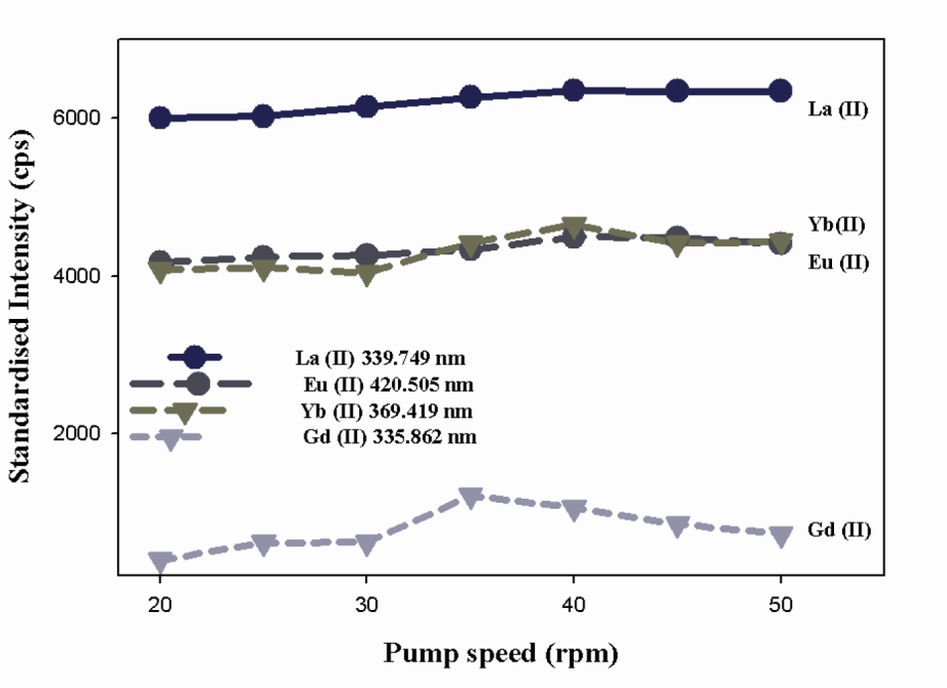


Figure 5. The effect of pump speed on 0.5 mg L^{-1} of La(II), Yb(II), Eu(II) and Gd(II) standardised intensity counts. The nebuliser gas flow rate was kept at 0.80 I/min and plasma power at 1300 W.

3.5. REEs optical transition

The REEs being a unique cluster of elements of atomic number from 57 to 71 increase in atomic number with a smooth decrease in ionic radius. This occurrence called lanthanide contraction applicable to all trivalent (triple positive charge) atoms makes the chemical properties of REEs very similar and hence they hold similar optical transitions [30]. The REEs have localised electrons that have interesting properties that originate from intraconfigurational transitions within the 4f level [31]. Due to high temperatures of the plasma (8000–10,000°C), there is a complete energy transfer in the form of emission and scattering of electromagnetic radiation. Er^{3+} and Yb^{3+} are examples of heavy rare earth elements with weak electron-phonon coupling, hence making emission simple because of the low energy involved and stable signals produced. The optimised conditions discussed in this chapter showed that different conditions give rise to variant optical transitions of the REEs as shown on plasma power of 1000–1600 W in **Table 3**. Detailed transitions of the REEs were outside the scope of this chapter.

3.6. Comparison of results in sediment samples

Two sediment samples, labelled VAD-01 and VAD-02 both collected from sampling sites near Durban harbour in South Africa, were taken for ICP spectroscopic analysis and the results are presented in **Table 3**.

3.6.1. Samples and reference material

The ICP results for two sediment samples, labelled VAD-01 and VAD-02, are presented in **Table 3**. The certified reference material GRE-03, a carbonatite from Tanzania rich in rare earth metals, was used to test the accuracy and recoveries. It should be noted that the matrix of this reference material does not fully match the sediments since we did not find a suitable sediment reference material with REEs. However, the reference material provided satisfactory results for the comparison of the three sample preparation techniques, fusion ICP-OES, acid ICP-OES and fusion ICP-MS analysis. The results obtained for the sample preparation technique provided further evidence that the different sample preparation techniques investigated were within the confidence limits of the results for reference material.

3.6.2. The comparison of results for two digestive methods investigated

The results obtained for the lithium metaborate fusion and four-acid digestion (HCl, HF, HNO_3 and $HClO_3$) procedures are expressed as the mean of three replicates as presented in **Table 3**. The solutions from both methods were analysed using the same conditions of the optimised ICP-OES procedure to determine the efficiency of the methods. The lithium metaborate digested samples were analysed on both ICP-OES and ICP-MS techniques to check the effectiveness of the optimised ICP-OES analysis conditions. The results of the heavy rare earth elements in **Table 3** from Sm to Lu clearly observed the Oddo-Harkins rule, which states that elements with even atomic number are more abundant than the elements with odd atomic number.

Element (ppm)	Wavelength (nm)	ICP-OES (Fus)	ICP-OES (4-acids) [VAD-01]	ICP-MS	ICP-OES (Fus)	ICP-OES (4-acids) [VAD-02]	ICP-MS	ICP-OES (Fus)	ICP-OES (4-Acids)	ICP-MS	Ref value (95% confidence interval)
La	333.749	26.2	23.4	25.8	31.3	27.3	30.9	2216.7	2078.3	2218.6	2224 ±36
Ce	418.660	40.5	35.8	38.7	65.1	56.7	59.8	4352.9	4236.4	4361.8	4354 ±29
Pr	417.939	10.9	10.5	11.2	7.2	6.6	7.1	490.3	414.3	488.7	496.6 ±8.9
Nd	430.358	1.2	1.0	0.7	31.5	32.8	30.9	1855.9	1847.3	1856.1	1835.9 ±33
Sm	360.428	10.7	9.8	8.1	7.0	5.8	7.3	269.7	251.0	276.8	279.4 ±4.9
Eu	420.505	0.8	ND	0.3	1.6	1.7	1.6	72.1	68.3	71.9	75.24 ±2.0
Gd	335.862	8.3	5.6	9.4	7.9	7.4	7.7	196.6	161.2	193.4	191 ±3.6
Tb	321.890	1.1	0.6	1.5	2.2	2.1	1.8	20.4	13.2	20.2	21.65 ±0.42
Dy	338.502	5.5	3.8	5.4	8.2	8.2	7.6	92.9	69.7	89.9	92.33 ±2.2
Ho	345.600	0.8	ND	0.6	0.7	0.4	0.8	12.1	5.1	12.4	13.53 ±0.33
Er	349.910	2.3	1.6	2.4	1.9	1.5	0.7	11.3	10.9	16.8	28.84 ± 0.52
Tm	313.126	ND	ND	0.1	0.2	ND	0.1	2.7	2.6	2.9	3.08 ± 0.1
Yb	369.419	2.3	2.0	1.9	4.9	4.2	5.1	16.1	13.5	14.8	15.5 ±0.24
Lu	261.542	0.2	ND	0.4	ND	ND	0.2	0.9	ND	1.3	1.81 ±0.1
Y	371.030	16.3	16.6	18.0	24.1	22.8	25.1	319.5	311.9	317.9	320.6 ±5.7

Table 3. Comparison of analytical results obtained for spectroscopic evaluation by fusion ICP-OES, acid ICP-OES and fusion ICP-MS analysis of sediment samples.

http://dx.doi.org/10.5772/intechopen.68280

The results obtained for the two samples and a reference material GRE-03 show enhanced results on most elements for the fusion method compared to the mineral acid digestion method. The acid digestion method does not completely dissolve some of the very resistant minerals and REEs, especially in hard rocks. Although the results are so close to that obtained in the fusion method, this can be attributed to the easy dissolution of the sediment material. The results suggest that the lithium metaborate fusion results in total dissolution of metals and is ideal for litho-geochemistry, including major oxides and trace rare earth metals. The detection limit of the acid digestion method was also compromised as we did not detect Eu, Ho and Lu in sample VAD-01, Tm in sample VAD-02 and Lu in sample GRE-03, but results were obtained for the fusion method. Generally, the acid digestion results for the GRE-03 sample was found to be lower than the certified values because of the difficulty in breaking the carbonatite in the sample matrix.

3.6.3. The comparison between ICP-OES and ICP-MS

The analytical techniques were performed using the same solution from the lithium metaborate fusion technique. The ICP-MS technique was found to be more efficient though costly in the trace elemental analysis, when compared to the ICP-OES technique. However, when comparing the results of ICP-MS with the optimised ICP-OES conditions, the former technique was very useful in validating the sediment results.

Most elements showed good agreement when the results are compared with less than 5% difference on all the samples analysed, including the reference material. For some elements with low levels present, such as Gd, Dy, Ho and Yb, the ICP-OES occasionally got slightly higher values than the ICP-MS technique. This observation in results was not significantly high, but it can be attributed to some spectral interferences.

The results obtained for the GRE-03 reference material compared well with the reported values listed in the table although the results for Ho, Tm and Lu were all moderately low on both instruments.

4. Conclusions

In this study, sample to flux ratio, optimum emission wavelengths, nebuliser flow rate, plasma power and pump speed were selected as major parameters to produce an analytical protocol for determining REEs in sediments. Of the two digestion procedures attempted, the more successful is obviously the flux-fusion method due to its ability of complete dissolution and simplicity due to automated fluxer fusion machine. The lower limit of detection was used as the optimisation criterion. The optimum values determined for sample to flux ratio, nebuliser gas flow rate, plasma power and pump speed (aspiration rate) were 1:8, 0.8 L min^{-1}, 1400 W and 35 rpm, respectively. The nebuliser gas flow was the most important parameter in the optimisation of the signal intensities. After optimisation of the parameters, the performance characteristics of the proposed method were established: linearity, detection and quantification limits and accuracy (recovery percentage), with and without addition of an internal standard.

Acknowledgements

Special thanks for the support provided by the research laboratory at Scientific Services consulting analytical laboratory (Cape Town). The authors also like to thank the National Research Foundation (South Africa) and the CSIR (NRE, Stellenbosch) for supporting this research. We further acknowledge the support of the SensorLab, Chemistry Department, University of the Western Cape, Bellville, South Africa. A word of thanks also to the Chemistry Department, Faculty of Applied Sciences, Cape Peninsula University of Technology, Bellville, South Africa.

Author details

Martin Makombe[1], Charlton van der Horst[2], Bongiwe Silwana[2,3], Emmanuel Iwuoha[2] and Vernon Somerset[4,*]

*Address all correspondence to: somersetv@cput.ac.za

1 Scientific Services Consulting Analytical Laboratory, Cape Town, South Africa

2 SensorLab, Department of Chemistry, University of the Western Cape, Bellville, South Africa

3 Department of Chemistry, Durham University, Durham, United Kingdom

4 Department of Chemistry, Faculty of Applied Sciences, Cape Peninsula University of Technology, Bellville, South Africa

References

[1] Chaillou G, Anschutz P, Lavaux G, Blanc G. Rare earth elements in modern sediments of the Bay of Biscay (France). Marine Chemistry. 2006;**100**:39-52.

[2] Ali SH. Social and environmental impact of the rare-earth industries. Resources. 2014; **3**(1):123-134.

[3] Makombe M, Van der Horst C, Silwana B, Iwuoha E, Somerset V. Antimony film sensor for sensitive rare earth metal analysis in environmental samples. Journal of Environmental Science and Health A. 2016;**51**(8):597-606.

[4] Zawisza B, Pytlakowska K, Feist B, Polowniak M, Kita A, Sitko R. Determination of rare earth elements by spectroscopic techniques: A review. Journal of Analytical Atomic Spectrometry. 2011;**26**:2373-2390.

[5] Hall GM, Pelchat JC, Loop J. Determination of zirconium, niobium, hafnium and tantalum at low levels in geological materials by inductively coupled plasma mass spectrometry. Journal of Analytical Atomic Spectrometry. 1990;**5**:339-349.

[6] Rivoldini A, Fadda S. Inductively coupled plasma mass spectrometric determination of low-level rare earth elements in rocks using potassium-based fluxes for sample decomposition. Journal of Analytical Atomic Spectrometry. 1994;**9**:519-524.

[7] Lotter SJ, Purcelll W, Nel JT, Snyders E. Alternative dissolution of zircon samples and simultaneous analysis of major and trace components. The Journal of the Southern African Institute of Mining and Metallurgy. 2012;**112**:69-76.

[8] Amaral CDB, Machado RC, Barros JAVA, Virgilio A, Daniela Schiavo D, Nogueira ARA, Nóbrega JA. Determination of rare earth elements in geological samples using the Agilent SVDV ICP-OES [Internet]. 2016. Available from: www.agilent/cs/library/applications/5991-692EN.pdf [Accessed: 21 October 2016].

[9] Li JX, Zhu ZW, Yin XF, Han B, Zheng L, Wang JT, Wang XR. Analysis of contents and distribution patterns of rare earth elements in the surface sediments of the south mid-Atlantic ridge. Chinese Journal of Analytical Chemistry. 2015;**43**(1):21-26.

[10] Bayon G, Barrat JA, Etoubleau J, Benoit M, Bollinger C, Revillon S. Determination of rare earth elements, Sc, Y, Zr, Ba, Hf and Th in geological samples by ICP-MS after Tm addition and alkaline fusion. Geostandards and Geoanalytical Research. 2009;**33**(1): 51-62.

[11] Claisse. Claisse M4 gas fusion user manual. Corporation Scientific Claisse Inc., Zurich, Switzerland 2010; 27-38

[12] Jin X, Zhu H. Determination of platinum group elements and gold in geological samples with ICP-MS using a sodium peroxide fusion and tellurium co-precipitation. Journal of Analytical Atomic Spectrometry. 2000;**15**:747-751.

[13] Obaje SO, Akpoborie IA, Ugbe FC, Onugba A. Rare earth and trace elements distribution in sediments of river Gora, Minna area, North-Central Nigeria: Implication of provenance. Earth Science Research. 2015;**4**(1):103-112.

[14] Zhang Y, Gao X, Chen CTA. Rare earth elements in intertidal sediments of Bohai Bay, China: Concentration, fractionation and the influence of sediment texture. Ecotoxicology and Environmental Safety. 2014;**105**:72-79.

[15] Panteeva SV, Gladkochoub DP, Donskaya TV, Markova VV, Sandimirova GP. Determination of 24 trace elements in felsic rocks by inductively coupled plasma mass spectrometry after lithium metaborate fusion. Spectrochimica Acta B. 2003;**58**:341-350.

[16] Ramteke DD, Annapurna K, Deshpande VK, Gedam RS. Effect of Nd^{3+} on spectroscopic properties of lithium borate glasses. Journal of Rare Earths. 2014;**32**(12):1148-1153.

[17] Bentlin FRS, Pozebon D. Direct determination of lanthanides in environmental samples using ultrasonic nebulization and ICP OES. Journal of Brazilian Chemical Society. 2010;**21**(4):627-634.

[18] Spectro analytical instruments [Internet]. 2016. Available from: www.spectro.com [Accessed: 11 November 2016].

[19] Agilent Technologies. AutoMax Fast automated method optimization, Technical Overview 700 Series ICP OES [Internet]. 2010. Available from: www.agilent.com/cs/library/technical overviews/public/si-0286.pdf [Accessed: 21 October 2016].

[20] Silva FV, Trevizana LC, Cintia Silva S, Nogueira Ana Rita A, Nobrega JA. Valuation of inductively coupled plasma optical emission spectrometers with axially and radially viewed configurations. Spectrochimica Acta B. 2002;**57**:1905-1913.

[21] Guimarães-Silva AK, de Lena JC, Froes RES, Costa LM, Nascentes CC. Evaluation of signal-to-background and Mg II/Mg I ratios as response for the optimization of rare earth elements determination by inductively coupled plasma optical emission spectrometry. Journal of Brazilian Chemical Society. 2012;23(4):753-762.

[22] Hou X, Jones BT. Inductive coupled plasma/optical emission spectrometry. Encyclopedia of Analytical chemistry, John Wiley and Sons Ltd, Chichester. 2000;9468-9485.

[23] Santos FN, Silva IS, Gomide RG, Oliveira LC. Evaluation of the rare earth impurities determination in Gd_2O_3 matrix by ICP-OES. In: International Nuclear Atlantic Conference – INAC; 24-29 November 2013; Recife, PE, Brazil. Associação Brasileira De Energia Nuclear – ABEN. ISBN: 978-85-99141-05-2.

[24] Bourmans PWJM. Measuring detection limits in inductively coupled plasma emission spectrometry using SBR-RSDB approach: A tutorial discussion of theory. Spectrochimica Acta. 1991;**46B**:431-445.

[25] Bourmans PWJM, Tielrooy JA, Muessen F. Mutual spectral interferences of rare earth elements in inductively coupled plasma atomic emission spectrometry: Rational line selection and correction procedure. Spectrochimica Acta. 1988;**43B**:173-199.

[26] Sturman BT, Doidge PS. Semi empirical approach to the calculation of instrumental detection limits in inductively coupled plasma atomic emission spectrometry. Journal of Analytical Atomic Spectrometry. 1998;**13**:69-74.

[27] Wu S, He M, Hu B, Jiang Z. Determination of trace rare earth elements in natural water by electrothermal vaporisation ICP-MS with pivaloyltrifluoroacetone as chemical modifier. Microchimica Acta. 2007;**159**:269-275.

[28] Barbalace K. Periodic table of elements sorted by 1st ionization potential(eV) [Internet]. 1995. Available from: www.environmentalchemistry.com/yogi/periodic/1stionization.html [Accessed: 28 October 2016].

[29] Boumans PWJM. Inductive coupled plasma emission spectroscopy, part1. Methodology, instrumentation and performance, John Wiley and Sons. New York, USA. 1987

[30] Castor SB, Hedrick JB. Rare earth elements. In: Kogel JE, Trivedi NC, Barker JM, Krukowski ST, editors. Industrial minerals and rocks – commodities, markets and uses. 7th ed. Society for Mining, Metallurgy and Exploration, Inc. (SME). Littleton, Colo. 2006. pp. 769-792.

[31] Knyazev Yu V, Noskov MM. The optical properties of rare earth metals. Physica Status Solidi (B). 1977;**80**:11.

IntechOpen

IntechOpen